

TABLE 1  
APERTURE PHOTOMETRY OF WARM SOURCES.

Identification	$R$ (mag)	$B - V$ (mag)	$B - R$ (mag)	$V - R$ (mag)	$V - I$ (mag)	$D_{25}$ (kpc)
IRAS 15015+1037 (I359)	13.91±0.01	0.24±0.01	0.63±0.01	0.39±0.01	0.71±0.01	18.2
	14.23±0.01	0.15±0.01	0.51±0.01	0.36±0.01	0.51±0.01	2
IRAS 04507+0358 (I156)	13.18±0.01	0.85±0.04	1.36±0.03	0.51±0.01	1.02±0.01	31.1
	14.32±0.01	0.93±0.01	1.45±0.01	0.53±0.01	1.08±0.01	2
IRAS 02580-1136 (I67)	13.16±0.01	0.40±0.10	1.28±0.10	0.88±0.01	...	43.1
	15.01±0.01	0.84±0.10	1.49±0.10	0.65±0.01	...	2
IRAS 03202-5150 (I80)	14.47±0.01	0.82±0.03	1.36±0.03	0.54±0.01	1.04±0.01	30.3
	15.83±0.01	0.88±0.01	1.37±0.01	0.48±0.01	0.99±0.01	2
IRAS 09497-0122 (I260) <sup>+</sup>	...	...	...	...	...	9.7*
04124-0803 (I114)	14.15±0.01	0.68±0.03	1.27±0.03	0.59±0.01	0.93±0.01	15.3
	14.40±0.01	0.71±0.01	1.37±0.01	0.65±0.01	0.96±0.01	2
IRAS 13512-3731 (I330)	14.80±0.01	1.00±0.03	1.57±0.03	0.57±0.02	1.04±0.02	12.1
	15.21±0.01	1.07±0.02	1.66±0.02	0.58±0.02	1.04±0.02	2
IRAS 15304+3017 (I375)	15.59±0.01	...	...	0.53±0.02	1.16±0.02	24.1*
	16.81±0.01	...	...	0.50±0.01	0.90±0.01	2
IRAS 04493-6441 (I153)	15.41±0.01	0.41±0.10	0.90±0.10	0.49±0.00	...	17.4
	16.43±0.01	0.29±0.10	0.77±0.10	0.49±0.00	...	2
IRAS 00521-7054 (I19)	15.56±0.01	...	1.098±0.10	...	...	32.7
	16.43±0.01	...	1.313±0.10	...	...	2
IRAS 09305-8408 (I254)	15.12±0.02	0.63±0.08	1.28±0.07	0.64±0.03	1.24±0.03	21.8
	16.14±0.01	0.93±0.08	1.62±0.03	0.69±0.02	1.32±0.01	2
IRAS 19580-1818 (I495)	14.88±0.02	0.80±0.04	1.14±0.05	0.35±0.03	1.17±0.03	14.0
(east nucleus)	15.69±0.01	0.85±0.03	1.29±0.03	0.44±0.02	1.35±0.02	2
(west nucleus)	16.30±0.02	0.59±0.04	0.88±0.04	0.29±0.03	0.95±0.03	2
IRAS 13536+1836 (I333)	13.40±0.07	0.61±0.10	1.31±0.10	0.70±0.09	...	37.1
(east nucleus)	15.22±0.07	1.45±0.10	1.59±0.11	0.14±0.09	...	2
(west nucleus)	15.78±0.08	0.55±0.10	1.05±0.10	0.50±0.09	...	2
IRAS 05136-0012 (I171)	12.61±0.01	...	...	0.47±0.01	...	46.4
	13.16±0.01	...	...	0.48±0.01	...	2
IRAS 03355+0104 (I96)	15.28±0.01	...	1.15±0.10	...	...	17.2
	15.94±0.01	...	1.12±0.10	...	...	2
IRAS 13144+4508 (I315)	15.12±0.07	0.25±0.10	0.98±0.10	0.73±0.08	...	41.1
	16.73±0.07	0.71±0.10	1.30±0.10	0.59±0.08	...	2
IRAS 22017+0319 (I528)	15.04±0.01	...	...	0.37±0.01	...	30.7*
	16.34±0.01	...	...	0.31±0.01	...	2
IRAS 20481-5715 (I512)	11.25±0.01	0.78±0.09	1.36±0.08	0.58±0.02	1.20±0.02	35.8
	12.69±0.01	0.87±0.08	1.49±0.08	0.62±0.02	1.28±0.02	2
IRAS 05218-1212 (I176)	...	...	...	...	1.02±0.08	30.6*
	...	...	...	...	0.79±0.08	2
IRAS 09182-0750 (I253)	...	...	...	...	1.07±0.08	29.2*
	...	...	...	...	1.32±0.08	2
IRAS 00509+1225 (I18)	13.51±0.01	0.22±0.09	0.56±0.08	0.33±0.02	0.73±0.02	28.6
	14.11±0.01	0.27±0.09	0.53±0.08	0.26±0.02	0.53±0.02	2
IRAS 21299+0954 (I521)	14.06±0.01	0.31±0.09	0.62±0.08	0.32±0.02	0.68±0.02	36.9
	14.54±0.01	0.24±0.09	0.47±0.08	0.22±0.02	0.50±0.02	2
IRAS 03059-2309 (I72)	13.86±0.02	0.47±0.10	0.93±0.11	0.46±0.04	0.98±0.04	38.1
	15.63±0.01	0.81±0.10	1.35±0.08	0.53±0.02	1.21±0.02	2
IRAS 03362-1641 (I98)	14.33±0.01	...	1.34±0.10	...	...	37.8

TABLE 1—*Continued*

Identification	$R$ (mag)	$B - V$ (mag)	$B - R$ (mag)	$V - R$ (mag)	$V - I$ (mag)	$D_{25}$ (kpc)
	16.08±0.01	...	1.64±0.10	...	...	2
IRAS 15599+0206 (I392)	...	...	...	...	0.96±0.08	31.0**
	...	...	...	...	1.08±0.08	2
IRAS 11298+5313 (I283)E	13.36±0.08	0.63±0.10	1.51±0.10	0.88±0.09	...	29.9
	14.22±0.08	0.81±0.10	1.70±0.10	0.89±0.09	...	2
IRAS 11298+5313 (I283)W	14.15±0.08	0.48±0.10	1.38±0.11	0.90±0.09	...	19.9
	14.67±0.08	0.74±0.10	1.67±0.11	0.94±0.09	...	2
IRAS 09453+5043 (I259)	14.47±0.08	...	...	0.80±0.08	...	24.0*
	15.24±0.08	...	...	0.91±0.09	...	2
IRAS 02366-3101 (I55)	14.21±0.01	0.37±0.08	0.77±0.08	0.39±0.02	0.94±0.02	35.5
	15.16±0.01	0.27±0.08	0.69±0.08	0.41±0.02	0.84±0.02	2
IRAS 23254+0830 (I555)	12.54±0.01	0.49±0.08	1.04±0.08	0.55±0.02	1.00±0.02	46.8
	14.70±0.01	0.69±0.08	1.06±0.08	0.37±0.02	0.98±0.02	2
IRAS 00321-0019 (I9)	15.11±0.01	...	...	0.59±0.01	...	28.3*
	17.00±0.01	...	...	0.64±0.01	...	2
IRAS 19254-7245 (I489)	14.45±0.01	0.71±0.08	1.29±0.08	0.58±0.02	1.25±0.02	37.4
(south nucleus)	16.64±0.01	0.99±0.08	1.92±0.08	0.93±0.02	1.54±0.02	2
(north nucleus)	17.28±0.01	0.80±0.08	1.47±0.08	0.67±0.02	1.31±0.02	2
IRAS 08277-0242 (I245)	14.32±0.08	...	...	0.88±0.09	...	29.9*
	15.39±0.08	...	...	0.88±0.09	...	2
IRAS 23016+2221 (I547)	13.81±0.01	0.47±0.08	0.99±0.08	0.52±0.02	1.19±0.02	26.8
	15.24±0.01	0.34±0.08	0.91±0.08	0.57±0.02	1.10±0.02	2

\*Diameter of the 25th mag arcsec<sup>-2</sup> isophote measured on the V image

\*\*Diameter of the 25th mag arcsec<sup>-2</sup> isophote taken from literature

+Saturated center. Surface photometry only

NOTE.—Total and Nuclear Magnitudes and Colours. Sources in order of decreasing  $\alpha_{(25,60)}$ .

# Multicolour Optical Imaging of IR-Warm Seyfert Galaxies.

## II. Optical and IR Properties and their Correlations

Eleni T. Chatzichristou

*Leiden Observatory, P.O. Box 9513, 2300 RA Leiden, The Netherlands*

*NASA/Goddard Space Flight Center, Code 681, Greenbelt, MD 20771*

### ABSTRACT

This paper is the second in a series, studying the optical properties of a sample of mid-IR Warm Seyfert galaxies and a control sample of mid-IR Cold galaxies. The present paper is devoted to aperture photometry. We discuss nuclear (within the central 2 kpc) and disk optical properties and their correlations with IR properties. We find a transition in the observed optical and IR properties from the Cold to the Warm Seyfert 2 and Seyfert 1 samples, with a partial overlap between the first two. This is in the sense of: (i) increasing nuclear optical luminosities and bluer nuclear colours (ii) decreasing disk optical luminosities and sizes (iii) increasing 25  $\mu\text{m}$  luminosities, decreasing far-IR excess ( $\frac{L_{FIR}}{L_B}$ ) and IR-loudness ( $\alpha_{(V,25)}$ ,  $\alpha_{(V,60)}$ ) and bluer  $\alpha_{(25,60)}$  and  $\alpha_{(12,100)}$  colours. We interpret these results as indicating larger dust content, and disk star formation for Seyfert 2s, while the optical properties of Seyfert 1s are mostly dominated by their nuclei. The 25  $\mu\text{m}$  emission of the Warm sample is mainly due to the AGN thermal component, although in Seyfert 2s it is probably further enhanced by disk star formation. Their far-IR (60-100  $\mu\text{m}$ ) luminosity on the other hand, traces mainly emission at large scales (host disks). In the Cold galaxies, the bulk of IR emission at all wavelengths appears to be dominated by dust in their disks.

*Subject headings:* galaxies: active, Seyfert, interactions, photometry

## 1. Introduction and Data Preparation

In Chatzichristou 2000 (hereafter Paper I) we have presented our sample of IR-Warm Seyferts, selected from the De Grijp et al. original sample of warm IRAS sources (De Grijp et al. 1987 and De Grijp et al. 1992) and a control sample of IR-Cold galaxies, that span similar redshift and luminosity ranges as the Warm sample. The basic data,  $B, V, R, I$  broad-band optical imaging and reduction procedures were summarized in Paper I. In the present Paper II we extract global photometric measures for the sample galaxies and compare the Seyfert 1 vs Seyfert 2 and the Warm vs Cold (sub)samples.

Among the 54 Seyfert galaxies in our Warm sample photometric measures are available for 33 objects and the results are presented in Table 1. Among the 16 galaxies in our Cold sample, we have photometric data for 14 of them, presented in Table 2. For the rest of the objects the observing conditions were too variable to derive accurate colours and thus are omitted from further discussion in the present paper. Through-out this paper (as in Paper I) the objects are identified with both their IRAS name and their serial number (with prefix I) in the original list (De Grijp et al. 1987).

The present paper is structured as follows: in Section 1 we summarize the data preparation and in particular the identification of the optical counterparts of the IRAS sources in the case of multiple systems. In Section 2 we describe the results of our aperture photometry, concentrating in intercomparisons between the (i) Warm Seyfert 1 and 2 subsamples and (ii) the Warm and Cold (sub)samples; we then summarize the main conclusions of that section. In Section 3 we do an exhaustive search of possible relations between optical and IR properties and intercompare the Warm and Cold (sub)samples. We summarize our main conclusions at the end of that section. We close in Section 4 with some concluding remarks in an attempt to understand the nature of IR-Warm seyferts based on our aperture photometry results.

### 1.1. Optical Identifications

Inspection of the broad-band data presented in Paper I shows a large number of closely interacting or double nucleus systems. It is important to identify which member of each system is the optical counterpart of the IRAS source. In the original list of warm sources (De Grijp et al. 1987), the optical counterparts

were identified using the Palomar Sky Survey and the ESO/SRC plates. The limited angular resolution on those plates often prevented detection of the duplicity of the sources. In fact, in some cases where the two members of an interacting system were resolved, the IRAS position lay between the two galaxies. The IRAS angular resolution varies between 0.5 arcmin (at 12  $\mu\text{m}$ ) to 2 arcmin (at 100  $\mu\text{m}$ ) and the positional accuracy depends on the source size, brightness and spectral energy distribution. To resolve the ambiguity for our sources, we have re-calculated the IRAS positional accuracy for all fields from the individual IR images (flux and position calibrated) extracted from the SRON IRAS database (Groningen, The Netherlands). Typically, accuracies are of the order  $\sim 10\text{-}30$  arcsec along each direction. For the (twelve) ambiguous cases, with more than one optical candidates for the IRAS identification, optical and IR positions were then compared. Details are given in Chatzichristou 1999. After this analysis, there were three remaining cases with ambiguous identification: the Warm IRAS 11298+5313 and the Cold IRAS 04530-3850 and IRAS 09406+1018 galaxies. For each of these systems, both members are retained as possible IRAS candidates and are included in subsequent analysis of our data.

### 1.2. Double Nucleus Systems

In both samples there is a number of galaxies where more than one nuclei are visible, embedded in a common envelope. Among the objects with photometric data, we have three such cases in the Warm sample: two Seyfert 2s, IRAS 13536+1836 (I333) and IRAS 19254-7245 (I489), one Seyfert 1, IRAS 19580-1818 (I495) and one Cold system, IRAS 07514+5327 (I231). IRAS 13536+1836 has been extensively studied in the past, its eastern Seyfert nucleus being a radio source and most probably the main source of IR emission (see *e.g.*, Chatzichristou and Vanderschueren 1995). The nature of the western nucleus is less clear, probably a lower ionization Seyfert or a LINER (previous reference). Consequently, although in our tables we are listing measures for both nuclei, in our histograms and plots we are only considering the east nucleus. The case of IRAS 07514+5327, is more ambiguous. Chatzichristou et al. 1998 showed that both condensations are extended and show H II-like spectra. In the above paper, arguments are given for the southern condensation to be the locus of the (highly obscured) galaxy nucleus. However, it is possible that

the northern condensation is the location of a second nucleus and thus, both are included in our analysis. There is one more ambiguous case among the Cold sample objects, IRAS 04265-4801, with a peculiar patchy morphology and several knots of emission in the central region. The brightest central knot is the dominant (if not unique) nucleus and thus the one used in our subsequent analysis. In the remaining two cases of Warm double nucleus objects listed above, we have used measures for both nuclei. In the histograms we adopt a mean value for the nuclear magnitudes and colours and in the rest of the plots we show data points for both nuclei, connected with a line. We use total magnitudes and colours for the system as a *whole*, since in none of the above cases we can distinguish two individual stellar systems. It is interesting that in these cases, the total magnitudes of the merger system are not significantly brighter than the mean total magnitudes for each sample and sometimes are actually fainter. Because of the relatively small number of double nucleus systems in our samples, the above assumptions are unlikely to affect our results from the statistical correlations.

## 2. Aperture Photometry Results

To obtain magnitudes and colours for our galaxies, we have used both (i) concentric circular apertures at specified radii and (ii) elliptical apertures with varying centers that were fitted to the galaxy's isophotes at increasing radii (the photometric algorithm used is described in Chatzichristou 1999). The two methods give sometimes significantly different results; detailed comparisons and discussion can be found in Chatzichristou 1999. A number of photometric corrections to the measured magnitudes were applied, that are described in detail, also in Chatzichristou 1999.

In Tables 1 and 2 we list magnitudes and colours for our sample objects with photometric information. These are referred to as “total” when measured within the  $\mu_B=25$  mag/arcsec<sup>2</sup> elliptical aperture and as “nuclear” when measured within an elliptical aperture of semi-major axis 2 kpc. The choice of the nuclear radius is somewhat arbitrary; large enough so as to not be affected by seeing effects and at the same time sufficiently small so that properties within this region should be dominated by the central nucleus. Magnitudes, colours and major axis scale lengths are corrected for Galactic extinction and relativistic ef-

fects as described in Chatzichristou 1999. The objects in Tables 1 and 2 are listed in order of decreasing mid-IR warmth  $\alpha_{(25,60)}$ . For each object, the first row represents total and the second nuclear magnitudes.

### 2.1. Seyfert 1 vs Seyfert 2 Galaxies

In Figures 1 and 2 we plot the fractional distributions of nuclear, disk and total (apparent) magnitudes and colours for the Warm Seyfert 1 and 2 subsamples and for the Cold sample. The subscript *disk* denotes colours and magnitudes within the annulus defined between semi-major axes 2 kpc -  $a_{25}$ . Filled histograms represent the Warm Seyfert 1 and 2 distributions and empty histograms the Cold galaxy distributions. The sample mean values are shown as vertical bars on the lower x-axes, as explained in the figure captions. The Table 3 lists median and mean values for all the measured quantities and the various subsamples.

Here are our main conclusions:

#### *Magnitudes*

(i) The nuclear magnitudes show a significant shift in their distributions: Seyfert 1 nuclei are brighter than their Seyfert 2 counterparts and there is a tendency for this discrepancy to increase as we progress to shorter wavelengths. The Student's T-test shows statistically different means for the two subsamples, while the K-S test shows that the hypothesis that the two distributions match remains less than 10% (not a statistically significant level) for all  $B, V, R, I$  magnitudes. The above result persists for both apparent and absolute magnitudes, confirming that there are no distance-selection effects for Seyfert types 1 and 2 in our sample. A straightforward interpretation of this result is, according to the orientation unification model, that in Seyfert 1s the AGN is visible while in Seyfert 2s it remains (partially) obscured by dust. Another possibility is however, that the Seyfert 1 nuclei are intrinsically brighter and bluer compared to the Seyfert 2 nuclei.

(ii) Although the distributions of disk luminosities are comparable between the two Seyfert subsamples there is consistently a tendency for the Seyfert 2 disks to be brighter, although not at a statistically significant level. If this tendency is however true, it could indicate larger star formation in the Seyfert 2 disks.

Another possibility is that the disk luminosity simply scales with the larger size of the Seyfert 2 host galaxies, which will be discussed below. None of these alternatives is however compatible with the orientation unification scheme for Seyferts.

(iii) The Warm Seyfert 1 and 2 galaxies have comparable *total* optical fluxes, the two opposite effects described in (i) and (ii) compensating for each other and this seems to be independent of (optical) wavelength. The F-Variance and the T-Student's test show indeed statistically similar variances and means for the two samples.

(iv) In Figure 3 we show mag-mag plots for our three samples. The trends described earlier are better visible here:

*Nuclear vs Disk:* Seyfert 2 nuclei tend to be fainter and to reside in brighter disks, than their Seyfert 1 counterparts. Also, for both samples nuclear and disk colours correlate (*i.e.*, brighter nuclei tend to reside in brighter disks) this relation being better defined and steeper for Seyfert 2s.

*Nuclear vs Total:* The tendency for the nuclear magnitudes to scale with total magnitudes is well defined in these diagrams, in particular for the Seyfert 1s indicating that their total optical fluxes are dominated by their nuclei.

### Colours

(v) The distributions of colours shown in Figure 2 indicate clear differences between the two Seyfert (sub)samples. The Seyfert 1s have bluer nuclear colours compared to the Seyfert 2 nuclei. A similar shift is seen for their total colours. For the disk colours any such shift is less pronounced if at all present, this indicating that the Seyfert total colours are mainly reflecting the colours within 2 kpc from the center, this being true in particular for the Seyfert 1s, as we shall show below. Moreover, these results indicate that the two Seyfert types must have dramatically different colour gradients. These will be indeed extensively discussed in Paper IV. The Student's T-test shows in general significantly different means for the distributions of nuclear and total colours for the two (sub)samples. Furthermore, the K-S test lends a 95% statistical significance to the hypothesis that the Seyfert 1 and 2 nuclear and total colour distributions are not drawn from the same parent population. The exception to this is a large overlap of the  $(V - R)$  nuclear colours, which however can be explained by the

contamination of the Seyfert 1  $R$ -band magnitudes by nuclear broad  $H_\alpha$  emission, preferentially reddening their  $(V - R)$  colours. Another possible effect is contamination of the  $V$ -band magnitudes by the  $[O III]_{4959,5007}$  emission lines, that are more likely to affect the (shorter baseline)  $(V - R)$  colours. This effect would lead to an artificially bluening of both the Seyfert 1 and Seyfert 2 colours by similar amounts, within the orientation unification scheme.

(vi) In Figure 4 we show nuclear vs disk and nuclear vs total colour-colour plots. There seems to exist a correlation between the nuclear and disk colours for the Warm Seyfert 2 galaxies (with the exception of the  $(V - I)$  colours;  $(B - R)$  correlation coefficient 0.47, at 0.07 significance level). A similar trend is seen for the  $(B - R)$  colours in Seyfert 1s. This basically indicates that redder Seyfert 2 nuclei reside in redder hosts, the most straightforward interpretation being that reddening due to dust affects similarly their nuclear and outer regions. In the nuclear vs total colour plots we find significant correlations for both samples that become very tight in the case of Seyfert 1s: the correlation coefficients (Spearman's test) for the  $(B - R)$  and  $(V - R)$  colour-colour plots are  $\sim 1$  and  $\sim 0.7$  for the Seyfert 1s and 2s, respectively, at significance levels better than 0.003. Thus, we find again that the Warm Seyfert total galaxy colours are dominated by their colours within 2 kpc from the nucleus, in particular in Seyfert 1s.

The most important effect depicted in Figure 4 is that, while the disk colours of both types 1 and 2 objects are mostly overlapping, the Seyfert 2 nuclei are significantly redder (by 0.1-0.6 mag) than the Seyfert 1 nuclei. In other words, the Seyfert 2s tend to have redder nuclei for similar disk colours. This is indeed consistent with the nuclear torus obscuration hypothesis for Seyferts. However, we have also shown that Seyfert 2 disks tend to be somewhat redder than their Seyfert 1 counterparts (by an average  $< 0.2$  mag) and that the Seyfert 2 disk and nuclear colours tend to correlate (Figures 2 and 4) with each other. These indicate that Seyfert 2s are systems with more overall reddening (larger amount of dust) than Seyfert 1s.

(vii) The dashed line in Figure 4 indicates the loci of similar nuclear and disk colours. Points lying to the right/left hand side of it indicate respectively redder/bluer nuclei compared to their surrounding disks. With the exception of the  $(V - R)$  colours (possible reasons for that are discussed above) all the other colour-colour diagrams show positive colour gradients

(*i.e.*, redder colours as a function of radius) for most Seyfert 1s and *opposite*, negative colour gradients for most Seyfert 2s. Colour gradients are the subject of Paper IV, where they will be discussed in detail.

### Host Sizes

(viii) In Figure 5 we show the distribution of major-axis diameters corresponding to the  $\mu_{25}$  isophotes, mostly measured on the  $B$ -band images and, when these were not available, on the  $V$ -band images. Inclusion of the latter in the above distributions causes only a small ( $\leq 1$  kpc) shift to lower values (for all the samples), but otherwise does not alter significantly the distributions. Median and mean values (both with or excluding the  $V$ -band diameters) are listed in Table 3. Note that we use *physical* (kpc) rather than apparent (arcsec) diameters. Although the two Seyfert samples have similar redshift distributions (see Figure 7), it is clear that the distribution of their diameters is not the same: Seyfert 1s are overall *smaller* than Seyfert 2s. This is probably related to the tendency we found earlier for Seyfert 1 galaxies to have fainter disks compared to the Seyfert 2 galaxies in our sample.

To investigate whether Seyfert 2 disks are brighter because they are larger or because their surface brightness is higher, we tried to correlate major-axis diameters vs magnitudes for all scales; some of these plots are shown in Figure 6. We do find a correlation between diameters and disk magnitudes, for both the Seyfert 1 and Seyfert 2 samples. Assuming an exponential disk, the flux should be proportional to  $h^2$  ( $h$  being the disk scale length) or alternatively to  $D^2$ . Thus, for constant central surface brightness  $\mu_0$ , the disk luminosity will scale with disk size as  $M_1 - M_2 = -5 \log D_1/D_2$ . In Figure 6 we have plotted this relation (arbitrarily shifted on the y-axis) as a dashed line. The correlation appears to be tighter for Seyfert 1s, roughly following the expected correlation between disk size and luminosity. Seyfert 2s show larger scatter and a clear deviation from the above curve: at the large- $D_{25}$  end, for similar-sized hosts Seyfert 2s have brighter disks than Seyfert 1s; at the faint-disk end, for similar brightnesses Seyfert 2 disks tend to be larger. This indicates that Seyfert 2 disks tend to be larger *and* brighter than their Seyfert 1 counterparts. Total magnitudes show some correlation with host sizes, for both samples, but with larger scatter.

Do *nuclear* magnitudes correlate with host dimen-

sions? In the same figure we show the  $V_{nuclear}$  vs  $D_{25}$  diagram. We do see a tendency for the brighter Seyfert 1 to reside in larger (and brighter) hosts, conclusion reached earlier from our mag-mag plots. We don't find this tendency for Seyfert 2s; instead, as we concluded earlier from our histograms, the Seyfert 2 nuclei tend to be fainter than their Seyfert 1 counterparts for similar host sizes. To investigate the possible origin for the different host properties between the two samples we have also plotted disk colours against sizes and luminosities. There is a tendency for Seyfert 1s disks, when bluer to also be larger (and brighter), which could be simply consistent with a sequence of earlier to later type hosts. Such a correlation is clearly not seen for the Seyfert 2s, one possible interpretation for this being the larger amount of dust residing in Seyfert 2 disks, as we concluded earlier from their redder colours.

In conclusion, in this section we have shown that there exist important differences between the Warm Seyfert 1 and 2 galaxies. If differences in their nuclear optical properties can be explained with larger torus obscuration of the Seyfert 2 nuclei, this is not the case for their host properties: We find that the Seyfert 2 host disks tend to be larger, brighter and redder, result that is difficult to accommodate within the simple orientation unification scheme for Seyferts. Inspection of the contour maps presented in Paper I, shows a larger fraction of interacting systems among the Seyfert 2 galaxies as compared to the Seyfert 1s. In Paper V we will investigate the correlation between host sizes/luminosities and the interaction statistics and find that there is indeed a good correlation between these two for the Seyfert 2 galaxies.

## 2.2. Warm vs Cold Samples

We have photometric information in the  $B, V, R$  bands for 14 out of 16 objects in the Cold sample (see Table 2). In this section we shall investigate how the distributions of various photometric properties compare between the Warm Seyfert and the Cold samples.

In Figures 1 and 2 we show the distributions of magnitudes and colours for the Warm (Seyfert 1 and 2) and Cold samples and in Table 3 we list the  $x$ [median and mean values for the Warm sample as a whole (and the two Seyfert subsamples) and for the Cold sample. As we will see in what follows, the Cold galaxies differ significantly from the Warm Seyfert 1s, while there is an overlap of properties between the former and the Warm Seyfert 2s. Our main results

are:

### *Magnitudes*

(i) Warm Seyferts tend to have brighter *nuclei* (Seyfert 1s by 1.5-2 mag, Seyfert 2s by  $\sim 0.5$  mag) than their Cold counterparts. The Student's T-test shows significantly different means (significance levels 0.006-0.03) for the Seyfert 1 and Cold samples and the K-S test shows that the null hypothesis for matching distributions can be rejected at a significance level better than 95%. On the other hand, there is a better overlap between the Warm Seyfert 2 and Cold nuclear magnitudes (statistically significant for the *B*-band) at shorter wavelengths, with a tendency for the Seyfert 2 nuclei to be brighter than their Cold counterparts (statistically significant for the *R*-band magnitudes).

(ii) There is an overlap in disk magnitudes between the Seyfert 2 and Cold samples (the K-S test shows matching distributions at significance levels better than 99% for the *B* and *R* magnitudes). The comparison is more ambiguous between Seyfert 1s and Cold galaxies, the latter tend to have brighter disks.

(iii) There is a general overlap in the integrated (total) colours for all three (sub)samples, statistically significant between the Seyfert 2 and Cold samples, in the case of *B* and *R* magnitudes.

(iv) In the magnitude-magnitude plots of Figure 3, the nuclear magnitudes of Cold galaxies (indicated with crossed squares) scale with disk (and total) magnitudes as in the case of the Warm Seyfert 2 sample. There is a good overlap between the Seyfert 2 and Cold objects in all wavelengths, but there are some Seyfert 2s clustering together with the Seyfert 1s. This ‘bimodality’ of the Seyfert 2 sample is best seen in the *R* mag-mag plot (larger number of points). The faintest Cold object in the *B* and *R* plots, is the southern member of the interacting system IRAS 09406+1018 (this is one of the systems for which both members are included in our analysis). Its isolation from the rest of the Cold sample might be indicating that the IRAS source is instead the brighter, northern component.

(v) In Figure 3 we indicate with **1** and **2** the Cold galaxies with observed Seyfert nuclear spectra. There are two more Seyfert 2s in our Cold sample but without photometric data. From the rest, five have H II-region like spectra and seven have no spectroscopic information (see Table 2 of Paper I). Although gen-

eral conclusions cannot be drawn from a small number of objects, it is interesting that (i) the two Cold Seyferts occupy similar places in these diagrams as their Warm counterparts and that (ii) the H II galaxies tend to overlap with the Seyfert 2 loci.

### *Colours*

(vi) The colour distributions for the three samples are shown in Figure 2 (there are only two Cold galaxies with simultaneous *B* and *V* band and none with *I* band measures). In Table 3, we list indicatively ‘median’ and ‘mean’ (*B* – *V*) colours. The Cold sample seems to span the whole (*B* – *R*) range covered by both the Warm Seyfert 1s and 2s. The colour distributions are different between the Cold and Seyfert 1 samples at all spatial scales (the former being redder) but there is an overlap in the (*V* – *R*) distributions between the Warm Seyfert 2 and Cold sample, that is statistically significant for the nuclear and total colours (K-S confidence level better than 95%). As we see in the colour-colour plots of Figure 4 the Cold objects span indeed the whole extend of the Warm sample colours. There is a good correlation between nuclear vs disk and nuclear vs total colours, as in the case of Seyfert 2s. Moreover, from the nuclear vs disk colour-colour diagram, we see that most Cold galaxies have negative colour gradients outwards, which we found to also be the case for the Warm Seyfert 2s.

### *Host Sizes*

(vii) In Figure 5 we show the distributions of major-axis diameters corresponding to  $\mu_{25}$ , for the Warm and the Cold samples. The distribution of Cold sample sizes is similar to that of Warm Seyfert 2s. On the mag vs  $D_{25}$  plots (Figure 6), we see a tendency for larger Cold disks to be also brighter (same tendency for their total magnitudes), with a large scatter around the expected correlation. In this figure we also find a good overlap between the Seyfert 2 and Cold samples and that the two Cold galaxies hosting a Seyfert nucleus have brighter nuclei *and* disks for similar host sizes, compared to the rest of the Cold sample.

## **2.3. Main Conclusions**

The optical properties of our sample objects suggest *intrinsic* differences between the IR-Warm Seyfert 1 and 2 hosts, as well as, a larger degree of nuclear obscuration in Seyfert 2s. Moreover, the Cold and



Warm Seyfert 2 samples show a significant overlap of properties. In particular, we find that:

(i) Seyfert 1 nuclei are brighter than their Seyfert 2 counterparts, this effect increasing at shorter wavelengths. Seyfert 1 nuclei are also bluer than Seyfert 2s for similar disk colours, this being probably the reason for the opposite colour gradients that we found in Seyfert 1s and Seyfert 2s (red/blue outwards, respectively). We can interpret these results as indicating either intrinsically brighter Seyfert 1 nuclei or larger obscuration of the Seyfert 2 nuclei.

(ii) Seyfert 2 disks are larger and brighter compared to their Seyfert 1 counterparts while the total magnitudes are similar for the two samples. The latter indicates that the Seyfert 1 optical properties are dominated by their nuclei and that Seyfert 1s are more compact than Seyfert 2s.

(iii) Extinction affects both the nuclei and hosts of Warm Seyfert 2s, that tend to be overall more dusty than Seyfert 1s (redder nuclear/disk/total colours).

(iv) There are no pronounced differences in the optical properties of the Warm (taken as a whole) and the Cold samples, except for a tendency of the Cold galaxies to be fainter and have redder nuclei. However, when comparing the Cold sample with the Seyfert 1 and 2 samples separately, we find that Cold galaxies are significantly different from the Warm Seyfert 1 galaxies as a sample, while there is a significant overlap in the optical properties (magnitudes, sizes and colours) of the Cold and Seyfert 2 samples.

### 3. Optical vs IR properties

#### 3.1. IR Fluxes and Colours

##### *Redshifts and IR Luminosities*

X[ In Figure 7 we show the distributions of 25 and 60  $\mu\text{m}$  luminosities and redshifts for the Warm Seyfert 1 and 2 and the Cold galaxies, with photometric information.

(i) As we showed in Paper I for the totality of the objects, all three samples occupy a similar range in redshifts. The only difference is the inclusion in the Warm sample of a few high-luminosity high- $z$  Seyfert 2 galaxies (see Paper I) in order to investigate the observed paucity of high-luminosity narrow-line AGNs.

(ii) A comparison of the distributions of the 25  $\mu\text{m}$  luminosities  $L_{25}$  shows significant differences between the three (sub)samples. The Warm Seyfert 1s span a

very narrow range in  $L_{25}$ , compared to the other two samples. Seyfert 2s tend to have larger 25  $\mu\text{m}$  luminosities than Seyfert 1s and, as expected, the Warm sample galaxies are brighter 25  $\mu\text{m}$  emitters than the Cold galaxies. The Student's T-test shows statistically significant different means between the Warm and Cold samples (significance level  $\leq 0.009$ ) and the K-S test shows that the null hypothesis that any of the Warm Seyfert and the Cold samples are drawn from the same population of 25  $\mu\text{m}$  luminosities can be rejected at a confidence level better than 96%.

(iii) The three samples span a similar range in 60  $\mu\text{m}$  luminosities. The Warm Seyfert 2 and the Cold galaxies have comparable distributions while the Warm Seyfert 1 distribution is shifted to somewhat lower luminosities (but with less than 95% statistical significance according to the K-S test).

How can these results be understood? Fadda et al. 1998 have found larger 25-100  $\mu\text{m}$  luminosities for type 2 nuclei compared to their type 1 counterparts, using an extended sample of Seyfert galaxies. They also found a similarly strong effect among UV-excess Seyferts but much weaker among IR-selected Seyferts. They concluded that it might be a selection effect, due to preferentially including in the optically selected samples Seyfert 2s with strong (mainly disk) star formation. Our samples include only Seyferts that were IR-selected but we find the same effect. In Paper I we have discussed a possible selection effect towards more powerful type 2 AGNs in our Warm sample, introduced by the optical spectroscopic classification of De Grijp et al. 1992. If this is true, it could explain the larger IR luminosities of these objects. However, in the same paper we showed that, on the basis of the IR colour selection criteria, it is unlikely that any low luminosity AGNs are included in the mid-IR Warm Seyfert samples, this being true for both Seyfert types. In turn, we suggest that the larger IR luminosities found for Seyfert 2s both in our sample and in those of Fadda et al. might indicate an *intrinsic* difference between the two classes of Seyferts. Possibilities are: (i) the mixed nature of Seyfert 2s (AGN plus starbursts), in which case the excess 25  $\mu\text{m}$  and 60  $\mu\text{m}$  emission is associated with excess star formation in Seyfert 2s, (ii) the larger (hot) dust content in Seyfert 2s, maybe related to recent interactions/mergers in these objects or (iii) differing contributions of the *nuclear* components of the 25  $\mu\text{m}$  emission (the AGN warming the dust more efficiently in Seyfert 2s, for some reason). Any one of these alter-

natives are difficult to reconcile with the simple torus obscuration model for Seyferts.

The modeling of thick dusty tori in Seyferts has shown that Seyfert 1s are expected to be stronger near- and mid-IR emitters (face-on tori) than Seyfert 2s, but to have similar far-IR luminosities. However, if the 25  $\mu\text{m}$  emission is mainly of nuclear origin, our result suggests that the tori are optically thin already at this wavelength. In Figure 8 we plot the  $\alpha_{(25,60)}$  vs  $\alpha_{(60,100)}$  colour-colour diagram for the Warm and Cold galaxies discussed in this paper (with photometric information). This plot illustrates the basic selection criterion  $\alpha_{(25,60)}$  between our Warm and Cold samples. The  $\alpha_{(60,100)}$  colour is commonly used as an indicator of dust heated by current star formation but it can also be affected by the cooler interstellar radiation field. For this reason, the  $\alpha_{(12,25)}$  is considered to be a better indicator of warm dust associated with star formation or/and an active nucleus. Thus, in Figure 8 we also show the  $\alpha_{(12,25)}$  vs  $\alpha_{(60,100)}$  colour-colour plot. Here, Seyfert 2s tend to have cooler (redder) 12-25  $\mu\text{m}$  colours than Seyfert 1s. This could be either the effect of the dusty torus being optically thick at  $\lambda < 25 \mu\text{m}$  (which we excluded earlier) or that Seyfert 2s are stronger 25  $\mu\text{m}$  IR emitters compared to Seyfert 1s, in favour of which we argued earlier. On the same colour-colour plot we find a tendency for cooler 12-25  $\mu\text{m}$  towards warmer 60-100  $\mu\text{m}$  colours, in particular for Seyfert 2s that tend to occupy the lower right part of the plot. Model predictions (*e.g.*, Xu & De Zotti 1989; Mazzarella et al. 1991) for non-Seyfert galaxies indicate that the relative importance and temperature of the warm dust component, related to star formation, increases as we progress from the upper left to the lower right corners of this diagram. Thus, the relative positions of our Warm subsamples suggest that Seyfert 2 galaxies have a larger fraction of warm dust related to increased star formation, compared to Seyfert 1s, while the generally warmer 12/25 colours of the latter indicate larger contribution of the nuclear component in these objects.

The distribution of IR luminosities for the Cold sample, shown in Figure 7, is shifted towards smaller 25  $\mu\text{m}$  and larger 60  $\mu\text{m}$  emission compared to the Warm sample and is easily understood in the context of our mid-IR colour criterion. In the  $\alpha_{(25,60)}$  vs  $\alpha_{(60,100)}$  colour-colour plot of Figure 8 the Warm and Cold samples are well separated by their  $\alpha_{(25,60)}$  colours (as was postulated by our main selection cri-

terion), while they span similar ranges in  $\alpha_{(60,100)}$  colours. On the  $\alpha_{(12,25)}$  vs  $\alpha_{(60,100)}$  colour-colour plot, Cold galaxies tend to segregate around intermediate values. Their colder 60-100  $\mu\text{m}$  colours compared to Warm Seyferts, for similar 12-25  $\mu\text{m}$  colours, indicate a significant contribution of colder dust at 100  $\mu\text{m}$  in these objects.

The narrow range of Seyfert 1 25  $\mu\text{m}$  luminosities that we found earlier, is more difficult to understand. One possible explanation for this would be their differing dust properties compared to the Seyfert 2s in our sample; if, for instance, we assume that in Seyfert 1s the AGN is the main source of mid-IR emission through thermal dust re-radiation, at some level of nuclear power and above, the small dust grains (responsible for the emission at this spectral range) tend to be destroyed. In Seyfert 2s this effect is less noticeable either because the central AGN is intrinsically fainter or because of the mixed nature (AGN+starburst) of their 25  $\mu\text{m}$  emission.

In conclusion, we can reconcile the differences of IR fluxes and colours between Seyfert 1 and 2 types, considering the alternatives (i) and (ii) mentioned earlier, *i.e.*, mixed nature (AGN+starbursts) and larger dust content for the Seyfert 2 galaxies. This however would lead to problems the simple obscuration picture, where the only difference between the Seyfert types should be their (projected) orientation on the sky.

### 3.2. IR Loudness Indices

The IR-loudness is defined by the optical-to-IR indices  $\alpha_{(V,25)} = 0.60 \log \frac{f_V}{f_{25}}$  and  $\alpha_{V,60} = 0.49 \log \frac{f_V}{f_{60}}$  where  $f$  denotes flux densities in units of Jy. The IR-loudness is primarily a measure of extinction and has been used as a warm dust indicator together with the  $\alpha_{(60,100)}$  colour index. Since we do not know the spatial extent of the mid-IR emission, we calculated the IR-loudness indices for both the nuclear and total  $V$  magnitudes and display their distributions in Figure 9 and their mean values in Table 4. Our main conclusions are:

(i) Seyfert 2 galaxies tend to be IR-louder than Seyfert 1s in all scales the difference being more pronounced and statistically significant for the nuclear indices and the 25  $\mu\text{m}$  IR emission: the Student's T-test shows that their means differ at significance level  $\sim 0.002$  and the K-S test shows that the null hypothesis that the two samples have matching distributions

of nuclear IR-loudness can be rejected at a significance level better than 95%. This result can be understood in terms of the larger optical extinction (in particular nuclear) and the stronger IR emission (in particular at 25  $\mu\text{m}$ ) found for Seyfert 2s.

(ii) The Cold galaxies are clearly IR-louder as far as the  $\alpha_{(V,60)}$  index is concerned, at all spatial scales. This is primarily due to the excess 60  $\mu\text{m}$  emission that characterizes the Cold sample (discussed earlier). The shift is more pronounced for the nuclear quantities, due to their fainter nuclear magnitudes (see Section 2.2). The Student's T-test shows that the mean values of  $\alpha_{(V,60)}$  differ significantly between the Warm Seyfert 1 and 2 and the Cold samples (significance  $\leq 0.005$ ) and the K-S test shows that the null hypothesis of matching distributions between either of the Warm and the Cold sample can be rejected at a significance level better than 95%.

(iii) There is a good overlap in the distributions of  $\alpha_{(V,25)}$  between the Warm and Cold samples. This is probably due to the competing effects of fainter  $V$  magnitudes for the Cold galaxies and larger 25  $\mu\text{m}$  excess for the Warm sample.

### 3.3. IR vs Optical Luminosities, Ionization and Host Sizes

#### $L_{IR}$ vs $L_{Optical}$

For a normal (non IR-luminous) galaxy, the far-IR luminosity (60-100  $\mu\text{m}$ )  $L_{IR}$  scales with blue luminosity  $L_B$  and galaxy size, because the IR traces dust heated by the older stellar population. The ratio  $\frac{L_{IR}}{L_B}$  tends to increase (there is an “excess”) when active star formation or an active nucleus are present. It follows that this ratio has often been used as a measure of the young/older stellar population dominance. However, it is not a very accurate indicator, if the IR and blue luminosities arise from different size areas; moreover, dust extinction would artificially increase this ratio. Having those in mind, in Figure 10 we plot  $L_{IR}$  vs  $L_B$  and  $L_R$ , nuclear and total, for the Warm and Cold samples. The main conclusions are:

(i) There is no obvious correlation between far-IR and nuclear optical luminosities for either of the Warm Seyfert samples. Seyfert 2s span a large range in  $L_{IR}$  for a relatively narrow range of *nuclear* optical magnitudes. The opposite trend is seen for Seyfert 1s (with the exception of one object).

(ii) We find a trend for  $L_{IR}$  to correlate with *total* optical luminosities for both Seyfert subsamples, sta-

tistically significant for the Seyfert 2s (correlation coefficient  $\sim 0.5$  with significance of the Spearman's rank test  $\sim 0.03$ ). The lack of any correlation between  $L_{IR}$  and nuclear optical luminosities seen above, indicates that the far-IR emission in Seyferts is dominated by warm dust in their host galaxy disk.

(iii) There is an overlap between Cold and Warm Seyfert 2 galaxies in these diagrams, but no obvious correlation between far-IR and optical luminosities for the Cold galaxies. This probably indicates important dust extinction at all spatial scales in the latter, that affects their optical luminosities. The two Cold galaxies with Seyfert nuclei are among the less IR bright among both the Cold and Warm samples.

(iv) At large IR luminosities, Seyfert 2s and Cold galaxies tend to be optically fainter compared to Seyfert 1s for similar  $L_{IR}$ . If this is the result of larger optical extinction, it would mean that the far-IR emission in the former objects scales with their dust content. This in turn, means that the  $\frac{L_{IR}}{L_B}$  ratio is also affected by dust extinction, especially at high IR luminosities ( $L_{IR} \geq 10^{11} L_{\odot}$ ).

(v) Having this in mind, we now compare the distributions of the  $\frac{L_{IR}}{L_B}$  ratio between the Warm Seyfert 1 and 2 and the Cold galaxies in Figure 11, calculated for both nuclear and total  $B$ -band magnitudes. We find indeed a larger  $\frac{L_{IR}}{L_B}$  ratio (excess IR to optical emission) for the Seyfert 2s compared to the Seyfert 1s, in particular for their *nuclear* blue luminosities (the K-S test shows that the two distributions are different at the 95% significance level). The Cold galaxies have similar  $\frac{L_{IR}}{L_B}$  distributions to those of the Warm Seyfert 2 sample (matching at the 97% significance level).

#### $L_{25}$ vs $L_{Optical}$

In Figure 12 we plot the  $L_{25}$  vs  $L_B$  and  $L_R$ , nuclear and total.

(i) As we saw earlier (Figure 7), Seyfert 1 nuclei occupy a very narrow strip in all diagrams, that is, they have similar 25  $\mu\text{m}$  luminosities for a wide range of optical luminosities (there is only one object, IRAS 00509+1225 (I18), that is detached from the rest of the sample towards higher  $L_{25}$ ). Consequently, Seyfert 1s show no correlation between 25  $\mu\text{m}$  and optical luminosities, at all wavelengths and spatial scales.

(ii) Seyfert 2 galaxies span a large range in  $L_{25}$ . Their 25  $\mu\text{m}$  luminosities show a definite correlation

with *total* (and disk) optical luminosities (correlation coefficient 0.7 with significance 0.004). Such a correlation is however not clear for their nuclear optical luminosities. This indicates that at least some of the 25  $\mu\text{m}$  emission in Seyfert 2s originates in their *host disks* while their nuclear regions remain highly obscured. The latter is further supported by the fact that in Figure 12 the Seyfert 2 nuclei are  $\sim 1$  order of magnitude fainter in the optical than their Seyfert 1 counterparts, for the whole range of 25  $\mu\text{m}$  luminosities. (The two galaxies detached somewhat from the Seyfert 2 sample by their lower  $L_{25}$ , are the two members of the interacting triple system IRAS 11298+5313 (I283)).

(iii) The Cold galaxies, occupy the lower left region in all the above diagrams, that is, towards lower 25  $\mu\text{m}$  and optical luminosities. They show large scatter and no obvious correlations. The two Cold Seyferts show the lowest  $L_{25}$  luminosities of all samples.

#### *IR luminosities vs Ionization*

We have considered possible correlations between IR luminosities ( $L_{IR}$ ,  $L_{25}$ ) and optical emission line fluxes and ratios ( $H_\alpha$ ,  $[\text{O III}]_{5007}$ ,  $[\text{O III}]_{5007}/H_\beta$ ), using spectroscopic (predominantly nuclear) data obtained by De Grijs et al. 1992. We can use those data only for the Warm Seyfert 2 sample, because the line fluxes for Seyfert 1s include contributions from both the broad and narrow Balmer components. As we have shown earlier, the mid- and far-IR emission in Seyfert 2s is probably dominated by dust in their host disks, consequently we do not expect any strong correlation between *nuclear* parameters and IR quantities. This is indeed the case as far as emission line fluxes are concerned, a result that agrees with the conclusions reached earlier by Keel et al. 1994 for the totality of the Warm sample. However we find a tendency for *anti-correlation* between both the far- and mid-IR fluxes and the ionization ratio  $[\text{O III}]_{5007}/H_\beta$ , which is shown in Figure 13. If true, this is an intriguing result and contradicts the correlation that Keel et al. 1994 found between the same ionization ratio and the IR-warmth  $\alpha_{(25,60)}$  index (for which we find no evidence in our subsample) and their conclusion, that both quantities are dominated by the AGN.

#### *IR Luminosities vs Host Sizes*

In Figure 14 we check the dependence of IR luminosity on galaxy size, represented by the major axis

length at  $\mu_B=25$  mag arcsec $^{-2}$ .

(i) There seems to exist a correlation between size and far-IR emission, for both Seyfert 1 and 2 types, but with large scatter (thus, not statistically significant). The two Seyfert 1 galaxies that deviate the most from this relation with over/underestimated diameters for their IR luminosities are IRAS 05136-0012 (I171) and IRAS 00509+1225 (I18), respectively. The *B*-band images of both objects are not very deep, consequently the extrapolation of their surface brightness profiles and their estimated diameters are less accurate. The same holds for the two Seyfert 2 galaxies with apparently underestimated sizes, for their IR luminosities (IRAS 09305-8408 (I254) and IRAS 15599+0206 (I392)). The Seyfert 2 galaxy that deviates from the correlation, with very large diameter for its IR luminosity is IRAS 02580-1136 (I67), due to its bright southern tidal arm.

(ii) The Cold sample shows a similar scaling between far-IR luminosity and host galaxy size, but this breaks down at the high end of  $L_{IR}$ , for four galaxies (IRAS 04454-4838, 23179-6929, 04530-3850 and 09406+1018) that are all members of closely interacting systems, tentatively suggesting that these objects tend to have larger far-IR excesses.

(iii) When plotting the 25  $\mu\text{m}$  emission vs galaxy size (same figure), we find no correlation for the Seyfert 1 galaxies, as expected if their 25  $\mu\text{m}$  emission is coming from the nuclear region, but a correlation (0.05 significance level) is seen for the Seyfert 2s.

### **3.4. IR Properties vs Optical Colours**

#### *IR Luminosities*

In Figure 15 we are plotting the  $L_{IR}$  luminosity and excess ratio  $\frac{L_{IR}}{L_B}$  vs optical colours, nuclear and total.

(i) We find large scatter in the plots involving  $L_{IR}$  and a tendency for Seyfert 1  $\frac{L_{IR}}{L_B}$  to correlate with redder colours, which can be explained if  $L_{IR}$  scales with galaxian light and the optical colours are affected by dust obscuration. No correlations are found for the Seyfert 2 or the Cold samples.

(ii) Seyfert type 1 and 2 galaxies occupy different regions in the above plots: from bluer colours and smaller IR excess for Seyfert 1s, to redder colours and larger IR excess for Seyfert 2s. As we discussed earlier this is probably due to larger dust extinction in the latter.

$\alpha_{(25,60)}$

There is no significant correlation between mid-IR warmness, expressed by this colour index and optical properties (luminosities or colours), except for a tendency for Seyfert 2 *nuclear* luminosities to have warmer (bluer) 25-60  $\mu\text{m}$  colours, shown in Figure 16. Mid-IR warmness does not correlate with either  $L_{IR}/L_B$ , galaxy size, or with any of the spectral (predominantly nuclear) properties of Seyfert 2s ( $H_\alpha$  emission, ionization ratio  $[\text{O III}]_{5007}/H_\beta$ , dust reddening  $H_\alpha/H_\beta$ ).

$\alpha_{(60,100)}$

We find no correlation between  $\alpha_{(60,100)}$  and optical properties for the Warm sample. On the other hand, the Cold sample shows a tight *anti-correlation* between far-IR colours and  $R$ -band total luminosities or host sizes. We also find warmer far-IR colours to scale with bluer optical colours (Figure 16), which could be explained if both are due to star formation. There is no significant correlation between  $\alpha_{(60,100)}$  and IR excess or optical spectral properties for any of the samples.

$\alpha_{(12,100)}$

In Figure 17 we plot the 12-100  $\mu\text{m}$  colour indices against various optical properties. The Warm and Cold samples are well-separated by this colour index, indicating that  $\alpha_{(12,100)}$  is a fairly good discriminator between AGN-dominated and normal/starburst-dominated galaxies. We find a correlation between warmer 12-100  $\mu\text{m}$  colours and *nuclear* optical luminosities for the Warm Seyfert 2 sample. There is also a tendency for cooler  $\alpha_{(12,100)}$  to correlate with nuclear extinction as measured by the  $H_\alpha/H_\beta$  ratio in Seyfert 2s. No significant correlations are found between  $\alpha_{(12,100)}$  and any optical properties, for the Warm Seyfert 1 galaxies. In fact, for these objects the  $\alpha_{(12,100)}$  colour spans a relatively narrow range for a large range in optical nuclear luminosities. A tendency exists for  $\alpha_{(12,100)}$  to correlate with nuclear optical luminosities for the Cold sample, as in the case of Seyfert 2s. We also find a trend for cooler  $\alpha_{(12,100)}$  with far-IR excess ratio  $L_{IR}/L_B$ .

These results indicate the nuclear origin of the 12  $\mu\text{m}$  emission in the Warm Seyfert 2 galaxies. On the plots of Figure 17 there is a continuous transition from cooler to warmer 12-100  $\mu\text{m}$  colours, fainter to brighter optical nuclear magnitudes, redder to bluer

optical nuclear colours and larger to smaller far-IR excess, as we progress from the Warm Seyfert 1, to the Warm Seyfert 2, to the Cold galaxies loci.

$\alpha_{(12,25)}$

Plots involving this colour show large scatter. No significant correlations were found between the  $\alpha_{(12,25)}$  colour index and any optical properties for any of the samples (*e.g.*, Figure 17).

### 3.5. IR Loudness vs Optical Properties

We have searched for trends/correlations between the IR-loudness indices,  $\alpha_{(V,25)}$  and  $\alpha_{(V,60)}$ , and various optical properties (Figure 18). We find:

(i) IR-louder Seyfert 1s tend to be optically fainter, the correlation holds for both nuclear and total magnitudes. This correlation is expected if the IR-loudness is primarily a measure of dust extinction. This seems to be confirmed by the tendency of IR-louder Seyfert 1s to have redder (nuclear and total) optical colours.

(ii) We find no such correlations for Seyfert 2s and even an opposite trend is found for IR-loudness to scale with *total* optical luminosities and bluer nuclear optical colours. We had seen earlier that the 25 (and 60)  $\mu\text{m}$  emission in Seyfert 2s correlates with optical luminosities and this is the most obvious reason for the IR-loudness correlations that we find here. We thus conclude that the *total* IR-loudness in Seyfert 2s is indicative of their IR emission rather than dust extinction. We can check these ideas also by plotting the IR-loudness indices vs nuclear reddening (as expressed by the spectral  $H_\alpha/H_\beta$  ratio) for Seyfert 2s. We find no significant correlation.

(iii) We have fewer points for the Cold sample and no clear trend could be defined from the above diagrams. On the IR-loudness vs nuclear optical luminosity diagram, there is a more or less continuous transition from the Cold and Seyfert 2 galaxies towards the Seyfert 1s as we progress from optically fainter and IR-louder towards brighter and less IR-loud nuclei.

All the trends/correlations described above hold for both IR-loudness indices but are better defined for the  $\alpha_{(V,25)}$  index.

(iv) As expected, the  $L_{IR}/L_B$  ratio is well correlated with the IR-loudness indices for all samples (not shown here), the correlation being particularly tight for the  $\alpha_{(V,60)}$  index.

(v) In Figure 18 we also plot the IR-loudness indices vs host galaxy size. We find a good correlation for Seyfert 1s in the sense, IR-louder objects tend to also be more compact. This is probably a consequence of the good correlation found earlier between optical *luminosities* and galaxy size. The same trend seems to exist for the Cold sample, although we have a smaller number of points. In the case of Seyfert 2s there is no clear correlation, which is expected since as we showed earlier both optical and IR luminosities correlate with galaxy size and between them, for these objects.

(vi) We find an anti-correlation between IR-loudness and the ionization ratio  $[\text{O III}]_{5007}/H_{\beta}$  for Seyfert 2s, which is expected since a similar anti-correlation was found earlier between this ratio and IR luminosity.

### 3.6. Main Conclusions

Comparison between the optical and IR properties of our samples lead to the following conclusions:

(i) Warm Seyfert 2 galaxies are stronger 25 and 60  $\mu\text{m}$  emitters, have a larger far-IR to optical excess  $\frac{L_{\text{IR}}}{L_B}$  and steeper (redder) 12-25  $\mu\text{m}$  and 25-60  $\mu\text{m}$  spectra, compared to Seyfert 1s. These differences suggest larger amounts of dust or/and larger contribution of star formation in Seyfert 2s, both indicating *intrinsic* differences between the two Seyfert classes.

(ii) In Seyfert 2s, the mid- and far-IR emission correlate with *total* optical luminosities and host galaxy sizes, this indicating that the bulk of IR emission in these objects is dominated by warm dust in the host galaxy disks. We find an anti-correlation between 25  $\mu\text{m}$  emission and nuclear ionization in Seyfert 2s, which is contradicting the simple orientation unification scheme where the 25  $\mu\text{m}$  emission is dominated by the AGN. At high IR powers, Seyfert 2s tend to be optically fainter than Seyfert 1s, for the same far-IR brightness, this being consistent with larger dust content in Seyfert 2s, especially at nuclear scales. Various correlations between IR colours and optical luminosities suggest that the 25-60  $\mu\text{m}$  emission in these objects is primarily originating in their disks. Shortward of 25  $\mu\text{m}$  their IR spectra are dominated by nuclear scales.

(iii) Seyfert 1s span a very narrow range in  $L_{25}$  over a large range in optical luminosities, with no obvious correlation between them at any spatial scales or wavelengths. The narrow 25  $\mu\text{m}$  emission range in these objects might be indicating the emitting

dust properties. The far-IR emission scales with *total* galaxian light and colours and with host size, this indicating that the Seyfert 1 far-IR emission is disk-dominated, as in the case of Seyfert 2s. There is no obvious correlation between the mid-to-far IR spectral shapes and the optical properties of Seyfert 1s, at any spatial scales.

(iv) Seyfert 2s are IR-louder, both at 25 and 60  $\mu\text{m}$ , compared to Seyfert 1s, especially at nuclear scales. IR-loudness correlates with brighter *total* optical luminosities and bluer *total* colours in Seyfert 2s, but with fainter optical luminosities and redder colours, at all spatial scales, in Seyfert 1s. In the latter objects, total IR-loudness also anti-correlates with host size. These results indicate that in Seyfert 1s IR-loudness is a measure of dust extinction and host luminosity, while in Seyfert 2s it is primarily indicative of IR excess emission at large scales and affected by dust extinction at nuclear scales.

(v) The Warm sample as a whole shows stronger 25 and weaker 60  $\mu\text{m}$  emission, compared to the Cold sample. Cold galaxies are IR-louder at 60  $\mu\text{m}$ , especially on nuclear scales. These results indicate both larger 60  $\mu\text{m}$  emission and nuclear dust absorption in IR-Cold galaxies. IR luminosities of Cold galaxies correlate with galaxy size, which indicates that their IR emission is dominated by warm dust in their disks. The closely interacting systems among them, tend to have larger IR excess. We find no significant correlations between the mid- or far-IR and optical luminosities of Cold galaxies, at all spatial scales. We interpret this as a result of dust extinction affecting their optical properties at all spatial scales. The 12-100  $\mu\text{m}$  colour index is as a good separator between Warm and Cold samples, as is the 25-60  $\mu\text{m}$  colour index and scales with  $\frac{L_{\text{IR}}}{L_B}$  in Cold galaxies. In Cold galaxies, the spectral shape at 12  $\mu\text{m}$  is correlated with nuclear optical properties, while longward of 60  $\mu\text{m}$  with their total optical properties. On the other hand we find no significant correlations involving the 25-60  $\mu\text{m}$  colour index in these objects.

(vi) In summary, we find a transition from fainter to brighter nuclear magnitudes, redder to bluer nuclear optical colours, redder to bluer 12-100 colours, larger to smaller  $\frac{L_{\text{IR}}}{L_B}$  and decreasing nuclear IR-loudness, as we progress from the Cold, to the Warm Seyfert 2 and to the Warm Seyfert 1 galaxies.

#### 4. Concluding Remarks

In this paper we presented the results of aperture photometry for our IR-Warm and Cold samples and discussed their optical properties (luminosities and colours, at various spatial scales and host sizes) in correlation with their IR properties (luminosities and colours). Our main conclusions are summarized in Sections 2.3 and 3.6. We find a transition in the observed optical and IR properties from Cold to Warm Seyfert 2 and Seyfert 1 galaxies, with a partial overlap between the first two.

Beginning to answer the two main questions that we formulated in Paper I, testing the universality of the orientation model and investigating the origin of mid-IR excess in Seyfert galaxies, our data so far indicates that: (i) Although some of the observed differences between the Warm Seyfert 1 and 2 samples (fainter and redder nuclei for the latter) could be accounted for by a preferential obscuration of the Seyfert 2 nuclei, other properties (larger and brighter Seyfert 2 disks) cannot, but rather indicate intrinsic differences between the two Seyfert types. In fact, the correlations between optical and IR properties indicate larger dust content and probably disk star formation in Seyfert 2s. (ii) The  $25\ \mu\text{m}$  emission in our Warm Seyferts is mainly due to the AGN thermal component, being further enhanced in Seyfert 2s by star formation. Their far-IR ( $60\text{--}100\ \mu\text{m}$ ) emission, on the other hand, originates in their host disks. In Cold galaxies, the bulk of IR emission at all wavelengths is dominated by warm dust in their disks, probably heated by strong star formation (at least in strongly interacting systems).

I am grateful to my thesis advisors George Miley and Walter Jaffe for providing me with stimulation and support throughout the completion of this project. This research has made use of the NASA/IPAC Extragalactic Database (NED) which is operated by the Jet Propulsion Laboratory, California Institute of Technology, under contract with the National Aeronautics and Space Administration. Part of this work was completed while the author held a National Research Council - NASA GSFC Research Associateship.

#### REFERENCES

Chatzichristou E.T. 2000, ApJ, submitted

- Chatzichristou E.T. 1999, PhD Thesis, Leiden Observatory
- Chatzichristou, E.T., Vanderriest, C., Lehnert, M. 1998, A&A, 330, 841
- Chatzichristou, E.T., Vanderriest, C. 1995, A&A, 298, 343
- De Grijp, M.H.K., Keel, W.C., Miley, G.K., Goudfrooij, P., Lub, J. 1992, A&AS, 96, 389
- De Grijp, M.H.K., Miley, G.K., Lub, J. 1987, A&AS, 70, 95
- Fadda, D., Giuricin, G., Granato, G.L., Vecchies, D. 1998, ApJ, 496, 117
- Keel, W.C., De Grijp, M.H.K., Miley, G.K., Zheng, W. 1994, A&A, 283, 791
- Mazzarella, J.M., Bothun, G.D., Boroson, T.A. 1991, AJ, 101, 2034
- Xu, C., De Zotti, G. 1989, A&A, 225, 12

TABLE 2  
APERTURE PHOTOMETRY OF COLD SOURCES.

Identification	$R$ (mag)	$(B - V)$ (mag)	$(B - R)$ (mag)	$(V - R)$ (mag)	$(V - I)$ (mag)	$D_{25}$ (kpc)
IRAS 07514+5327 (I231)	12.92±0.07	0.39±0.10	1.16±0.10	0.77±0.09	...	36.0
(north nucleus)	15.13±0.07	0.61±0.10	1.15±0.10	0.54±0.09	...	2
(south nucleus)	14.97±0.07	0.66±0.10	1.20±0.10	0.54±0.09	...	2
IRAS 06506+5025 (I211)	13.54±0.08	0.70±0.10	1.49±0.10	0.79±0.09	...	15.3
	14.40±0.08	0.54±0.10	1.50±0.10	0.95±0.09	...	2
IRAS 02439-7455 (Fairall11)	13.98±0.01	...	0.53±0.10	...	...	24.6
	14.59±0.01	...	0.46±0.10	...	...	2
IRAS 04015-1118 (NGC1509)	12.90±0.01	...	0.87±0.10	...	...	28.6
	13.80±0.01	...	0.75±0.10	...	...	2
IRAS 05217-4245 (ESO252-G022)	13.27±0.01	...	1.64±0.10	...	...	44.4
	15.36±0.01	...	1.96±0.10	...	...	2
IRAS 04265-4801 (ESO202-G023)	12.20±0.01	...	1.34±0.10	...	...	31.8
	14.33±0.01	...	2.05±0.10	...	...	1
IRAS 10475-1429 (MGC02-28-009)W	14.14±0.01	...	1.35±0.10	...	...	29.5
	15.96±0.01	...	1.52±0.10	...	...	2
IRAS06+1018 (CGCG063-051)N	15.56±0.01	...	0.77±0.10	...	...	34.0
	17.54±0.01	...	1.12±0.10	...	...	2
IRAS 09406+1018 (CGCG063-051)S	16.74±0.02	...	1.56±0.10	...	...	5.5
	17.19±0.01	...	1.66±0.10	...	...	2
IRAS 04530-3850 (ESO304-IG029)N	14.60±0.01	...	...	0.58±0.01	...	30.3*
	17.34±0.01	...	...	0.62±0.01	...	2
IRAS 04530-3850 (ESO304-IG029)S	14.61±0.01	...	...	0.43±0.02	...	34.1*
	15.76±0.01	...	...	0.49±0.01	...	2
IRAS 03531-4507 (ESO249-IG028)	15.02±0.01	...	0.85±0.10	...	...	31.7
	16.44±0.01	...	0.85±0.10	...	...	2
IRAS 04304-5323 (ESO157-IGA040)N	15.09±0.01	...	...	0.56±0.01	...	35.8*
	17.27±0.01	...	...	0.65±0.01	...	2
IRAS 04454-4838 (ESO203-IG001)N	15.89±0.01	...	...	0.48±0.01	...	21.5*
	17.19±0.01	...	...	0.47±0.01	...	2
IRAS 23179-6929 (ESO077-IG014)	14.62±0.01	...	...	0.66±0.01	...	25.9*
	15.98±0.01	...	...	0.80±0.01	...	2
IRAS 05207-2727 (ESO487-IG006)	14.42±0.01	...	1.50±0.10	...	...	33.3
	16.32±0.10	...	1.86±0.10	...	...	2

\*Diameter of the 25th mag arcsec<sup>-2</sup> isophote measured on the  $V$  image

NOTE.—Total and Nuclear Magnitudes and Colours. Sources in order of decreasing  $\alpha_{(25,60)}$



TABLE 3  
MEDIAN AND MEAN QUANTITIES FOR ALL SAMPLES.

Quantity	Median				Mean			
	Seyfert 1	Seyfert 2	Warm	Cold	Seyfert 1	Seyfert 2	Warm	Cold
$B_{nuc}^1$	15.85	16.98	16.81	17.29	15.92	16.83	16.49	16.90
$V_{nuc}$	15.27	16.27	15.69	16.78	15.27	16.15	15.82	16.79
$R_{nuc}$	15.16	15.83	15.24	15.98	14.88	15.59	15.33	15.91
$I_{nuc}$	14.48	15.33	14.71	...	14.37	14.96	14.66	...
$B_{25}^2$	14.97	15.54	15.42	15.03	15.25	15.19	15.21	15.25
$V_{25}$	14.60	15.03	14.68	15.20	14.59	14.65	14.63	15.08
$R_{25}$	14.15	14.33	14.32	14.60	14.17	14.17	14.17	14.34
$I_{25}$	13.66	13.78	13.66	...	13.63	13.32	13.47	...
$B_{disk}^3$	16.45	15.81	16.16	15.68	16.25	15.53	15.80	15.67
$V_{disk}$	15.69	15.17	15.39	15.47	15.56	15.03	15.23	15.38
$R_{disk}$	15.20	14.83	15.18	14.89	15.09	14.59	14.77	14.74
$I_{disk}$	14.68	13.89	14.23	...	14.53	13.65	14.09	...
$(B - V)_{nuc}$	0.29	0.87	0.81	0.63	0.42	0.88	0.70	0.59
$(B - R)_{nuc}$	0.77	1.49	1.37	1.50	0.89	1.46	1.24	1.36
$(V - R)_{nuc}$	0.49	0.62	0.57	0.62	0.49	0.60	0.56	0.65
$(V - I)_{nuc}$	0.84	1.21	1.04	...	0.79	1.16	0.97	...
$(B - V)_{25}$	0.41	0.63	0.49	0.70	0.46	0.59	0.54	0.55
$(B - R)_{25}$	0.90	1.29	1.27	1.34	0.94	1.25	1.13	1.19
$(V - R)_{25}$	0.49	0.59	0.57	0.60	0.49	0.65	0.59	0.61
$(V - I)_{25}$	0.94	1.07	1.02	...	0.90	1.09	0.99	...
$(B - V)_{disk}$	0.51	0.49	0.49	0.82	0.51	0.49	0.50	0.58
$(B - R)_{disk}$	0.99	1.24	1.11	1.26	1.00	1.16	1.10	1.16
$(V - R)_{disk}$	0.50	0.58	0.56	0.59	0.49	0.66	0.59	0.59
$(V - I)_{disk}$	1.04	1.07	1.04	...	1.07	1.08	1.07	...
$D_{25}[B + V]$	26.8	31.0	30.7	31.7	26.15	32.06	29.80	30.45
$D_{25}[B]$	28.9	35.8	32.2	31.8	27.01	33.34	30.81	30.92

<sup>1</sup>Within 2 kpc from the nucleus

<sup>2</sup>Within elliptical apertures corresponding to  $\mu_B=25$  mag arcsec

<sup>3</sup>Within the annulus defined between the above apertures

TABLE 4  
MEAN IR-LOUDNESS INDICES.

Quantity	Seyfert 1	Seyfert 2	Warm	Cold
$\alpha_{(V,25)}[25]$	-1.11	-1.23	-1.18	-1.12
$\alpha_{(V,25)}[\text{nuc}]$	-1.27	-1.59	-1.47	-1.53
$\alpha_{(V,60)}[25]$	-1.02	-1.13	-1.09	-1.40
$\alpha_{(V,60)}[\text{nuc}]$	-1.16	-1.43	-1.32	-1.74

NOTE.—The subscripts [nuc] and [25] refer to  $V$  magnitudes measured within the central 2 kpc and  $\mu_B = 25$  mag arcsec<sup>-2</sup> respectively (see text).

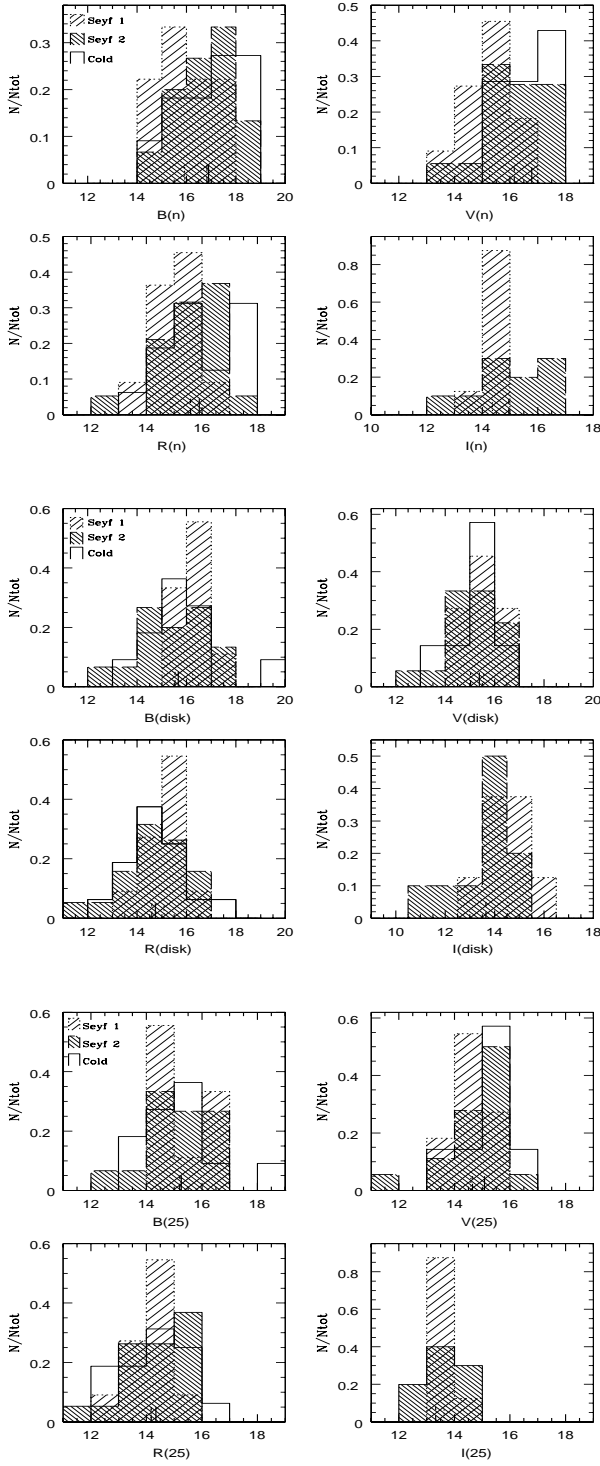


Fig. 1.— Fractional distributions of nuclear, disk and total apparent magnitudes, for the Warm Seyfert 1 and 2 and the Cold subsamples. Mean values are indicated as dotted, dashed and solid vertical bars, respectively, on the lower x-axes.

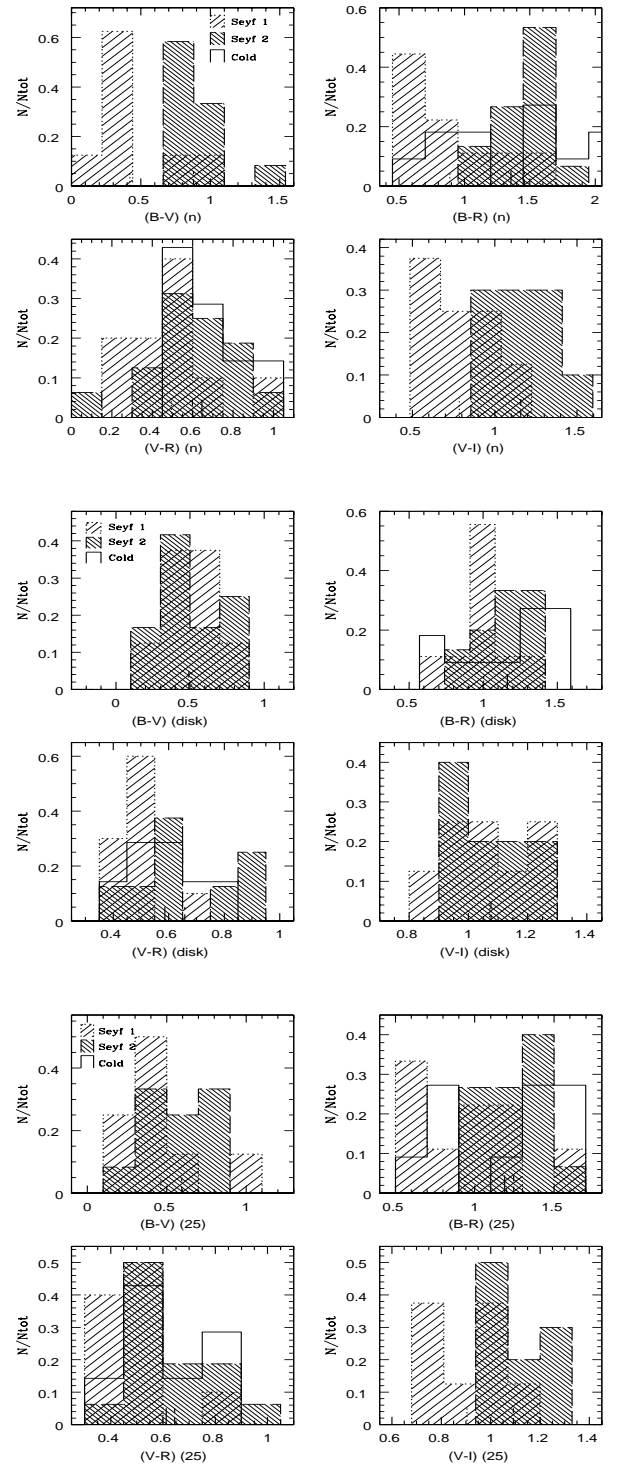


Fig. 2.— Fractional distributions of nuclear, disk and total colours, for the Warm Seyfert 1 and 2 and the Cold subsamples. Mean values are indicated as dotted, dashed and solid vertical bars, respectively, on the lower x-axes.

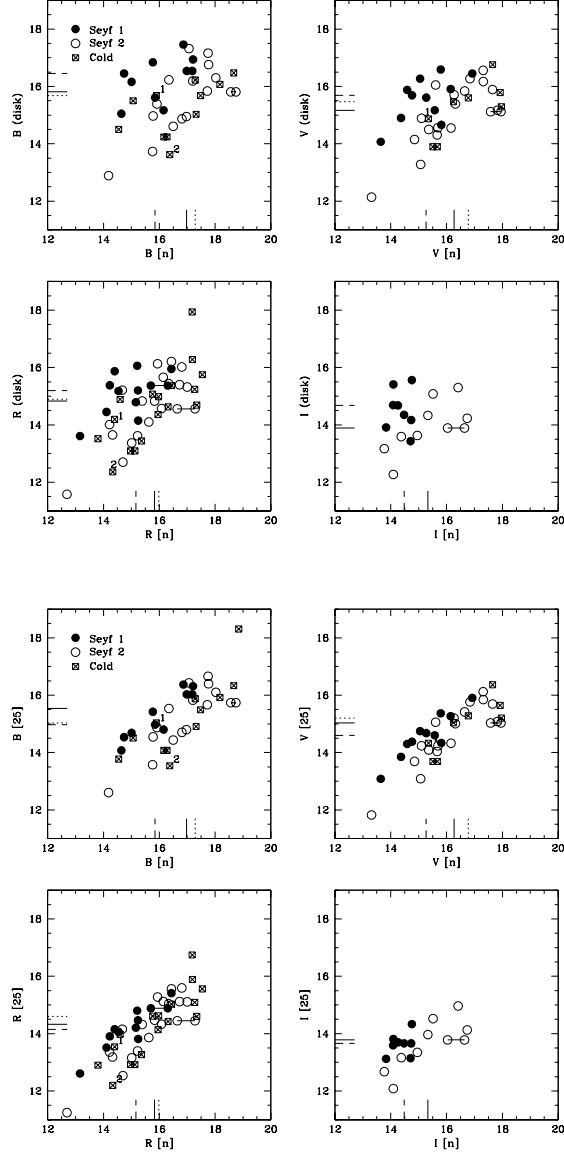


Fig. 3.— Nuclear vs Disk and Nuclear vs Total mag-mag plots for the Warm Seyfert 1 and 2 type galaxies and for the Cold sample. Horizontal lines connect measures for the two nuclei of double nucleus systems. Labels 1 and 2 indicate Seyfert type 1 and 2 nuclei within the Cold sample galaxies. Bars indicate median values (to be compared with the mean values indicated in the histogram plots) for the three samples: dashed for Seyfert 1s, solid for Seyfert 2s and dotted for the Cold galaxies.

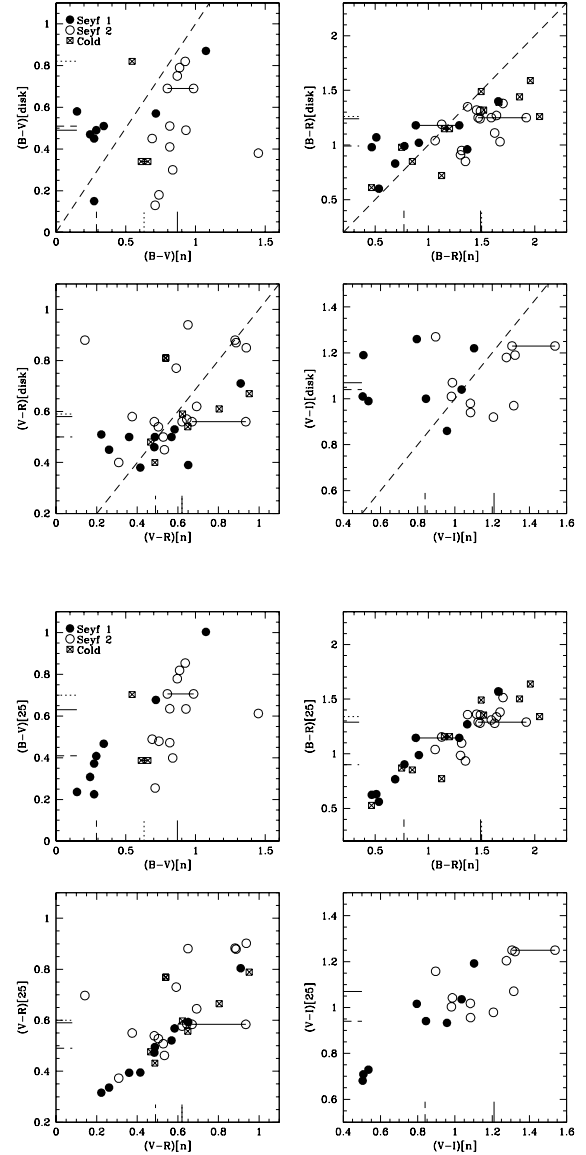


Fig. 4.— Nuclear vs Disk and Nuclear vs Total colour-colour plots for the Warm Seyfert 1 and 2 type galaxies and for the Cold sample. Horizontal lines connect measures for the two nuclei of double nucleus systems. Labels 1 and 2 indicate Seyfert type 1 and 2 nuclei within the Cold sample galaxies. Bars indicate median values for the three samples: dashed for Seyfert 1s, solid for Seyfert 2s and dotted for the Cold galaxies. Dashed lines indicate the loci of equal nuclear and disk colours.

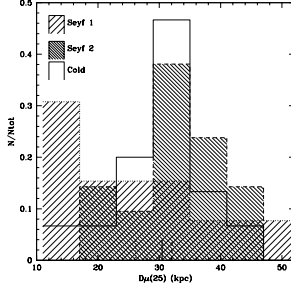


Fig. 5.— Fractional distributions of major axis diameters, measured within the isophote corresponding to  $\mu_B=25$  mag arcsec $^{-2}$ , for the Warm Seyfert 1 and 2 and the Cold samples. Mean values are indicated by the dotted, short and long solid vertical bars, respectively, on the lower x-axis.

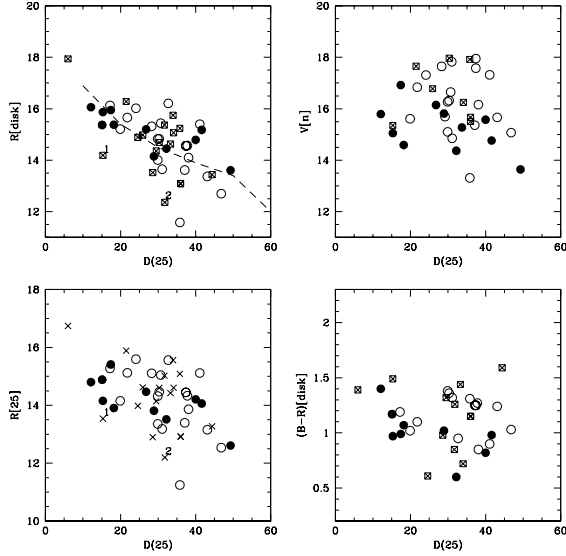


Fig. 6.— Major axis diameters, corresponding to  $\mu_B=25$  mag arcsec $^{-2}$  plotted against nuclear, disk and total magnitudes and disk colours. The dashed line indicates the expected correlation if disk luminosity scales with size (see text). The labels 1 and 2 indicate the types of Seyfert galaxies belonging to the Cold sample.

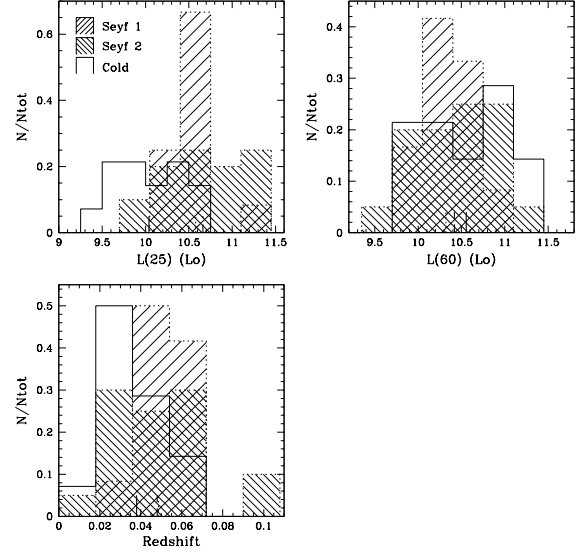


Fig. 7.— Fractional distributions of the 25 and 60  $\mu$ m flux densities and the redshifts, for the Warm type 1 and 2 Seyferts and the Cold sample (only the objects with photometric information). The vertical bars on the lower x-axes indicate mean values (dotted for Seyfert 1s, dashed for Seyfert 2s and solid for Cold galaxies).

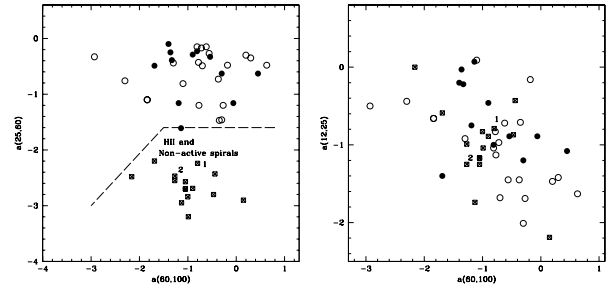


Fig. 8.— Mid- and far-IR colour-colour diagrams. Filled/open circles indicate Warm Seyfert 1s and 2s, respectively and crossed squares indicate the Cold galaxies. The labels 1 and 2 indicate the respective types of Seyfert nuclei within the Cold sample. The dashed line on the left panel approximately divides the AGN and normal galaxy regions according to the mid-IR colour selection criterion of De Grijp et al. 1987.

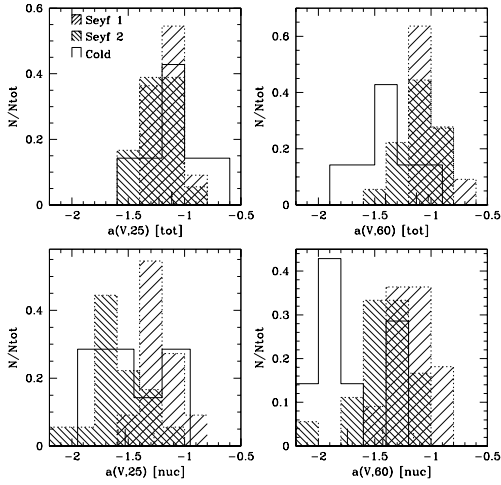


Fig. 9.— Fractional distributions of the  $\alpha_{(V,25)}$  and  $\alpha_{(V,60)}$  IR-loudness indices for the Warm Seyfert 1 and 2 and the Cold galaxies, with photometric information. The vertical bars on the lower x-axes indicate mean values for the two subsamples (dotted for Seyfert 1s, dashed for Seyfert 2s and solid for Cold objects).

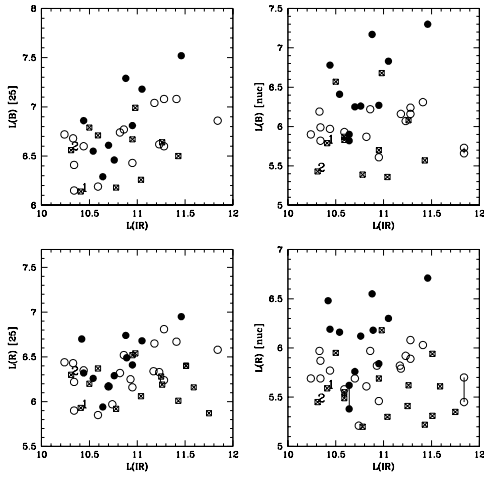


Fig. 10.— Far-IR (60-100  $\mu\text{m}$ ) vs optical (nuclear and total) luminosities for the Warm Seyfert 1 and 2 subsamples (filled/empty circles, respectively) and for the Cold sample galaxies (crossed squares). Solid lines connect points corresponding to the two nuclei of double nucleus systems. The labels 1 and 2 indicate the respective Seyfert types of Cold sample galaxies. Luminosities are expressed in solar units  $L_{\odot}$ .

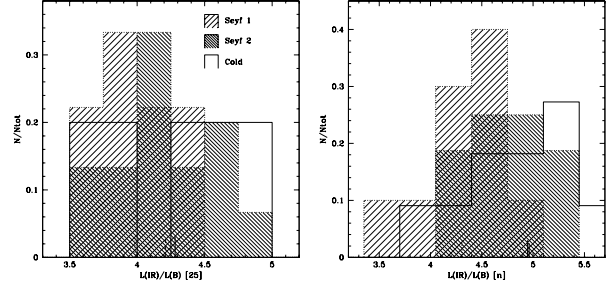


Fig. 11.— Fractional distributions of the  $\frac{L_{IR}}{L_B}$  ratio between the Warm Seyfert 1 and 2 and the Cold samples. The vertical bars on the lower x-axes indicate mean values for each subsample (dotted for Seyfert 1s, dashed for Seyfert 2s and solid for Cold objects).

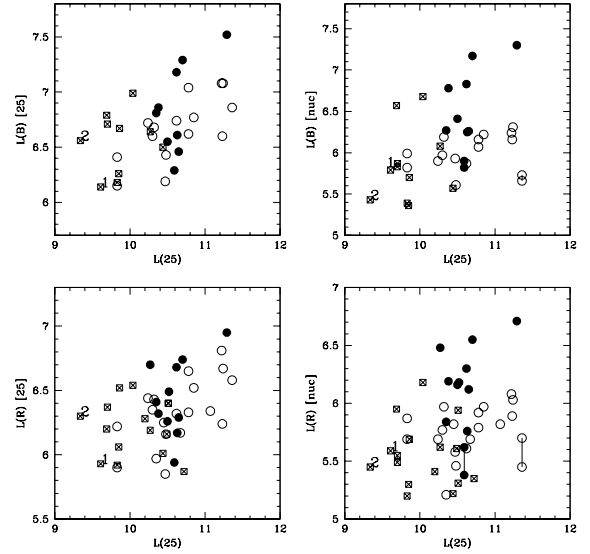


Fig. 12.— Mid-IR (25  $\mu\text{m}$ ) vs optical (nuclear and total) luminosities for the Warm Seyfert 1 and 2 (filled/empty circles, respectively) and the Cold samples (crossed squares). Solid lines connect points corresponding to the two nuclei of double nucleus systems. The labels 1 and 2 indicate the respective Seyfert types of Cold sample galaxies. Luminosities are expressed in solar units  $L_{\odot}$ .

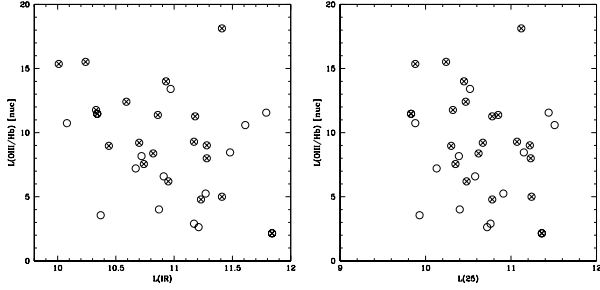


Fig. 13.— Mid- and far-IR luminosities against the ionization ratio  $[O\ III]_{5007}/H_{\beta}$ , for the totality of our Warm Seyfert 2 subsample. The crossed circles indicate objects for which we also have photometric information. Luminosities are in solar units  $L_{\odot}$ .

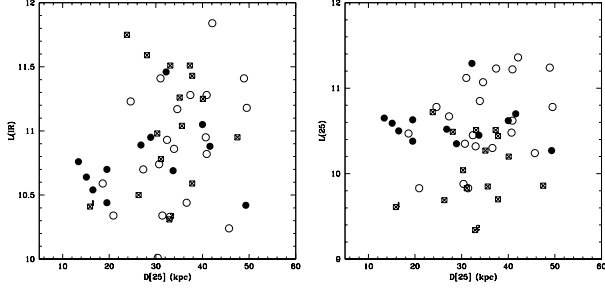


Fig. 14.— Mid- and far-IR luminosities against 25 mag arcsec $^{-2}$  diameters, for the Warm and Cold samples. Filled/open circles represent Warm Seyfert 1/2 galaxies and crossed squares Cold galaxies. The labels 1 and 2 indicate the corresponding nuclear types of Cold Seyferts. Luminosities are in solar units  $L_{\odot}$ .

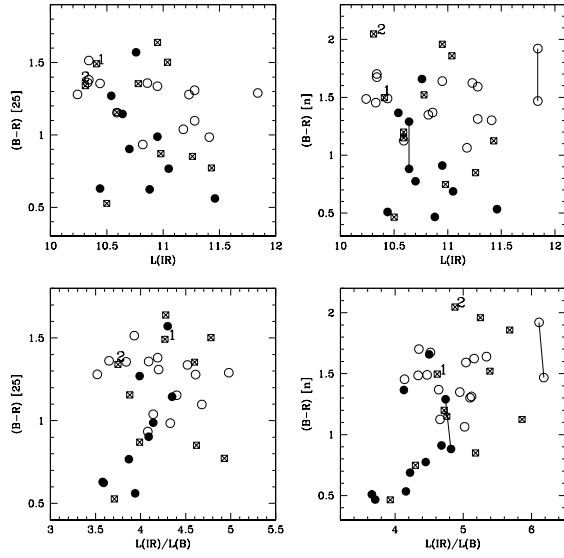


Fig. 15.— Far-IR (25-60  $\mu\text{m}$ ) luminosities and excess ratio  $\frac{L_{\text{IR}}}{L_B}$  vs optical (nuclear and total) colours for the Warm Seyfert 1 and 2 subsamples (filled/empty circles, respectively) and the Cold sample galaxies (crossed squares). Solid lines connect points corresponding to the two nuclei of double nucleus systems. The labels 1 and 2 indicate the respective Seyfert types of Cold sample galaxies. Luminosities are in solar units  $L_\odot$ .

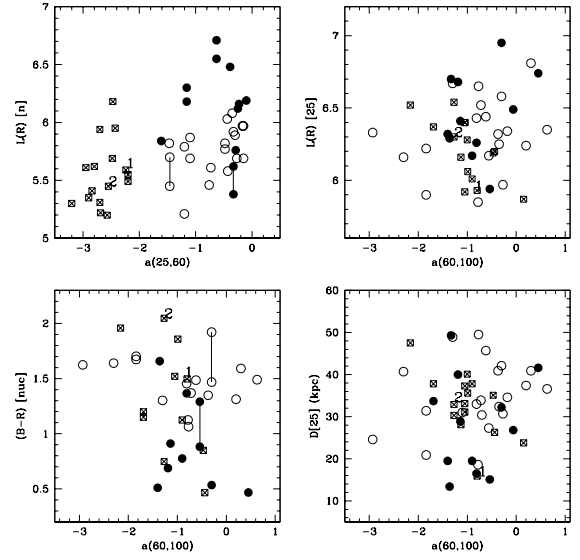


Fig. 16.— IR colour indices vs optical luminosities, nuclear ( $L_R(n)$ ) and total ( $L_R(25)$ ), nuclear ( $B-R$ ) colours and host sizes  $D_{25}$ , for the Warm Seyfert 1 and 2 subsamples (filled/empty circles, respectively) and the Cold sample galaxies (crossed squares). Solid lines connect points corresponding to the two nuclei of double nucleus systems. The labels 1 and 2 indicate the respective Seyfert types of Cold sample galaxies. Luminosities are in solar units  $L_\odot$ .



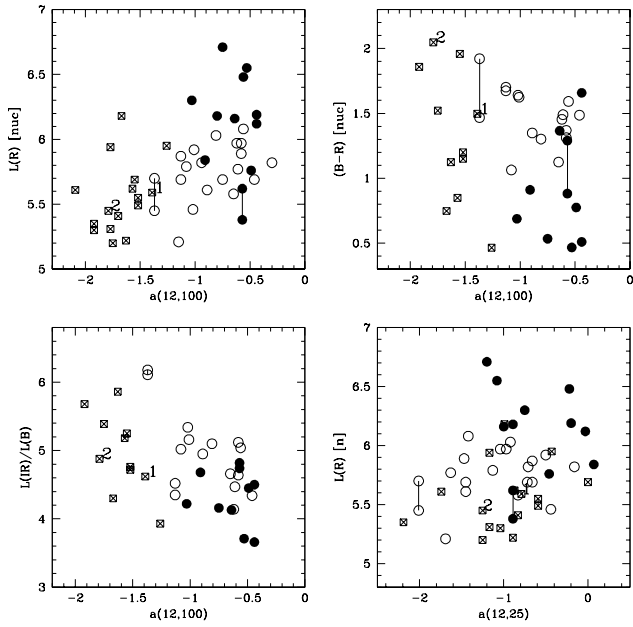


Fig. 17.— IR colour indices vs nuclear luminosities ( $L_R(n)$ ) and  $(B - R)$  colours and IR/optical excess ( $L_{IR}/L_B$ ), for the Warm Seyfert 1 and 2 subsamples (filled/empty circles, respectively) and the Cold sample galaxies (crossed squares). Solid lines connect points corresponding to the two nuclei of double nucleus systems. The labels 1 and 2 indicate the respective Seyfert types of Cold sample galaxies. Luminosities are in solar units  $L_\odot$ .

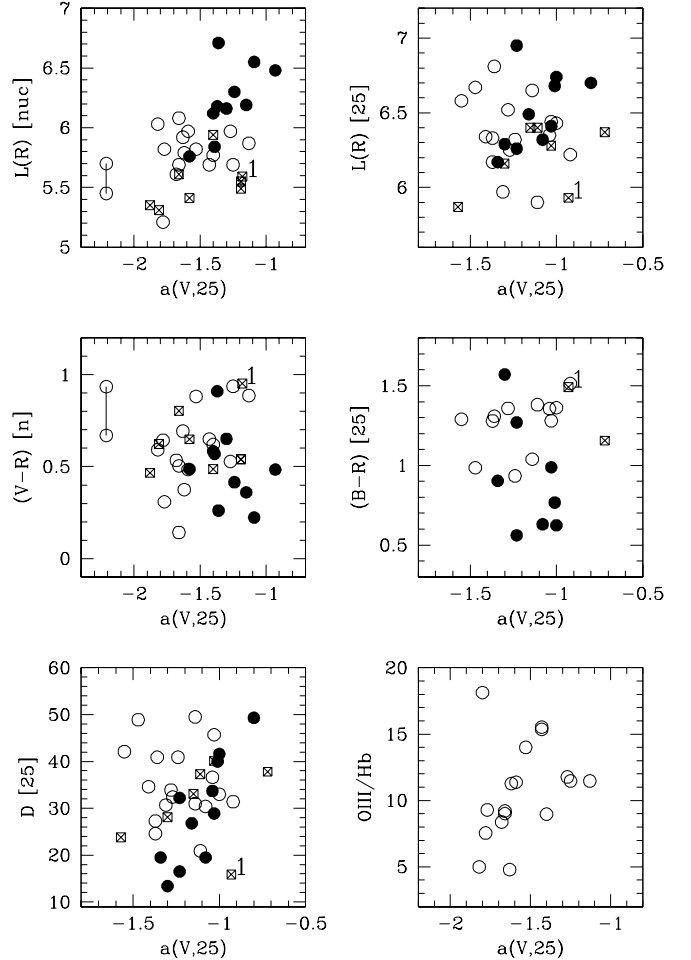


Fig. 18.— IR-loudness indices vs optical luminosities  $L_R$  and colours, nuclear and total, host size ( $D_{25}$ ) and ionization ratio  $[O\ III]/H_\beta$ , for the Warm Seyfert 1 and 2 subsamples (filled/empty circles, respectively) and the Cold sample galaxies (crossed squares). Solid lines connect points corresponding to the two nuclei of double nucleus systems. The labels 1 and 2 indicate the respective Seyfert types of Cold sample galaxies. Luminosities are expressed in solar units  $L_\odot$ .